Heat transfer in the thermo-electro-hydrodynamic convection under microgravity conditions

Mireille Tadie Fogaing, Harunori Yoshikawa, Olivier Crumeyrolle, Innocent Mutabazi

EPJ manuscript No.
(will be inserted by the editor)

Heat transfer in the thermo-electro-hydrodynamic convection under microgravity conditions

M. Tadie Fogaing[1], H.N. Yoshikawa[1a], O. Crumeyrolle[1], and I. Mutabazi[1b]

Laboratoire Ondes et Milieux Complexes, UMR 6294 CNRS, Université du Havre
53, rue de Prony, CS80540, 76058 Le Havre Cedex, France

Received: date / Revised version: date

Abstract. This article deals with the thermal convection in a dielectric fluid confined in a finite-length capacitor with a temperature gradient under microgravity conditions. The dielectrophoretic force resulting from differential polarization of the fluid plays the role of buoyancy force associated with an electric effective gravity. It induces the convection when the Rayleigh number based on this electric gravity exceeds a critical value. Two-dimensional numerical simulation for a geometry with a large aspect ratio is used to determine the convective flow in the saturated state. The Nusselt number Nu is computed for a wide range of Prandtl number ($0.01 \leq Pr \leq 10^3$) and its dependence on the distance from the critical condition is determined. A correlation between Nu and Pr in the vicinity of the criticality is obtained and compared with that of the Rayleigh-Bénard convection. The behavior of the convection is analyzed in detail from an energetic viewpoint: electrostatic energy, power inputs by different components of the electric gravity and viscous and thermal dissipations are computed.

PACS. 44.24.+f Natural convection – 47.65.-d Magnetohydrodynamics and electrohydrodynamics

1 Introduction

Rayleigh-Bénard (RB) convection in a fluid layer confined between two horizontal plates with a vertical temperature gradient along the gravitational acceleration has become the prototype of modern nonlinear physics [1–3]. Similar thermal convections can be induced by external fields other than the gravity by using specific properties of fluids. A magnetic field applied to ferrofluids [4] or an electric field applied to dielectric fluids [5] allow to generate a ponderomotive force which can be regarded as thermal buoyancy in an artificial gravity. The resulting convection intensifies the heat transfer, even in the absence of the Earth's gravity. Use of these artificial gravity is therefore of particular interest in applications in microgravity conditions, e.g., in orbital systems, in space factories.

In the present work, we are interested in the thermal convection induced by an electric field and a temperature gradient, both applied to a dielectric fluid. This convection is often referred to as thermo-electro-hydrodynamic (TEHD) convection [6]. It has been the subject of many investigations since few decades, particularly for the case of a dielectric fluid confined between two horizontal parallel plane electrodes [6–10]. The driving force of the convection is the dielectrophoretic (DEP) force. Its density is given by $\boldsymbol{F}_{DEP} = -\frac{1}{2}\boldsymbol{E}^2\boldsymbol{\nabla}\epsilon$, where $\boldsymbol{E}$ is the electric field and ϵ is the electric permittivity of the fluid. The DEP force is a consequence of differential polarization of the fluid. It is a component of the electrohydrodynamic (EHD) force [11,12] and dominates over the other components when the accumulation of free charges in the fluid is negligible and when the fluid is incompressible and has no mobile boundaries [10,13]. The charge accumulation occurs over a time scale of the charge relaxation time $\tau_e = \epsilon/\sigma$ (σ: the electric conductivity of the fluid) [13]. When the electric field is alternating with a frequency high compared with τ_e^{-1}, the fluid is free from the charge accumulation and the DEP force is the dominant EHD force component.

Under a temperature gradient, the DEP force is generated through the thermal variation of $\epsilon = \epsilon(T)$:

$$\boldsymbol{F}_{DEP} = -\frac{1}{2}E^2\boldsymbol{\nabla}\epsilon\,(T) = -\alpha\rho\theta\boldsymbol{g}_e + \boldsymbol{\nabla}\left(\frac{e\theta\epsilon_1\boldsymbol{E}^2}{2}\right), \quad (1)$$

where $\epsilon(T)$ has been modeled by a linear relationship $\epsilon(T) = \epsilon_1(1-e\theta)$ with the permittivity ϵ_1 at a reference temperature $T = T_0$ and the temperature deviation $\theta = T - T_0$. The coefficient e is positive and of the order of 10^{-3}–$10^{-2}\,\mathrm{K}^{-1}$ for most dielectric fluids. The density and the thermal expansion coefficient of the fluid are denoted by ρ and α, respectively. In eq. (1), the electric gravity $\boldsymbol{g}_e$ has been introduced, which is proportional to the gradient of

[a] *Present address:* Laboratoire J.-A. Dieudonné, UMR 7351 CNRS, Université Nice-Sophia Antipolis
[b] *E-mail:* innocent.mutabazi@univ-lehavre.fr

the electric energy stored in the fluid:

$$\boldsymbol{g}_e = \frac{e}{\rho\alpha}\boldsymbol{\nabla}\left(\frac{\epsilon_1 \boldsymbol{E}^2}{2}\right). \tag{2}$$

The first term in the right-hand-side of eq. (1) is the thermoelectric buoyancy associated with $\boldsymbol{g}_e$, which is the analogue of the Archimedean buoyancy. It can drive convective flow even in a thermal stratification stable against the Earth's gravity $\boldsymbol{g}$, i.e., in the configuration where the temperature gradient is directed opposite to $\boldsymbol{g}$ [6–8]. The second term in eq. (1) can be lumped with the hydrodynamic pressure term in the momentum equation.

One can find a qualitative similarity between the TEHD convection and the RB convection. Indeed, the TEHD convection develops, when the thermal buoyancy force overcomes viscous and thermal diffusion effects [6–8,14], as in the RB convection. The control parameter is the Rayleigh number L based on the electric effective gravity $\boldsymbol{g}_e$, as is the Rayleigh number R in the RB convection. However, the behavior of these convective flows is different from each other quantitatively. The critical state of the TEHD convection is characterized by the critical values of the electric Rayleigh number and wavenumber, $(L_c, k_c) = (2128.7, 3.226)$ [6,8,10,14], while the critical Rayleigh number and wavenumber of the RB convection are $(R_c, k_c) = (1708, 3.117)$ [15]. Stiles *et al.* [16] and Yoshikawa *et al.* [10] have examined the nonlinear behavior of the TEHD convection in the vicinity of the critical state by a weakly nonlinear analysis and by a two-dimensional direct numerical simulation (DNS), respectively. Their results have shown quantitative differences from the RB convection in saturated states. In particular, the heat transfer increases with the supercriticality $(L-L_c)/L_c$ more slowly in the TEHD convection than it does in the RB convection with $(R-R_c)/R_c$. The origin of these quantitative differences is attributed to the fact that, in the TEHD convection, the electric gravity is not constant but has a perturbative component $\boldsymbol{g}'_e$ resulting from the perturbation in electric fields. This perturbation electric gravity stabilizes the conductive state of the fluid and impedes the convection [10,17].

The scope of the present study is the extension of our recent work [10] and the development of the nonlinear properties of the TEHD convection in a two dimensional capacitor. A detailed analysis is performed on perturbation fields obtained by DNS from an energetic viewpoint. We discuss the aspects related to the electrostatic energy stored in the fluid, the viscous and thermal dissipations. Visualizations of the corresponding fields are also carried out. The heat transfer intensification by convection is examined over a range of the Prandtl number ($0.01 \leq Pr \leq 10^3$) wider than in the previous work ($1 \leq Pr \leq 10^3$). A correlation between the Nusselt number and the Prandtl number is determined and compared with the correlation for the RB convection.

The paper is organized as follows: in the next section, we present the flow equations and the numerical solution procedure. The results of the DNS are given and analyzed in sect. 3. The heat transfer enhancement is discussed in sect. 4. The last section is concerned with the conclusion.

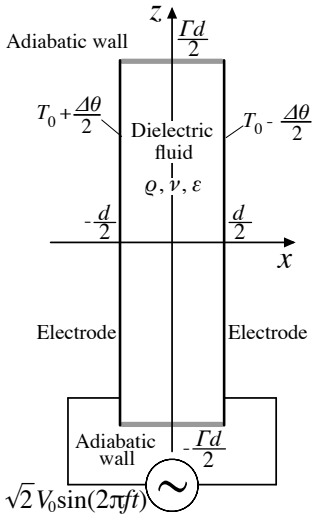

Fig. 1. Geometrical configuration of the problem

2 Flow equations

We consider a dielectric fluid confined in a capacitor with a temperature gradient and an alternating voltage $V(t) = \sqrt{2}V_0 \sin(2\pi f t)$ imposed over the gap between the electrodes (fig. 1). The frequency f is assumed high enough to neglect charge accumulation, but low enough for the electrostatic approximation: $\tau_e^{-1} \ll f \ll \ell/c$, where ℓ is the size of the capacitor and c is the speed of light. We also assume that the frequency is high compared to the inverse of the viscous relaxation time $\tau_\nu = d^2/\nu$. Then, the high frequency alternating component of the DEP force is filtered out by the viscous relaxation and only the static component of the DEP force should be taken into account in the flow calculation. The static component is determined from effective electric field $\boldsymbol{E}_0$, which is associated with the actual alternating field by $\sqrt{2}\boldsymbol{E}_0 \sin(2\pi f t)$. This time-averaged description has been used in the theoretical works on the TEHD convection [7–10,18]. A recent theoretical investigation showed that the description is valid when $2\pi f \tau_\nu \gtrsim 100$ [19].

In the EHD Boussinesq approximation [7], the governing equations are the following continuity, momentum and heat conduction equations:

$$\boldsymbol{\nabla}\cdot\boldsymbol{u} = 0, \tag{3}$$

$$\frac{\partial \boldsymbol{u}}{\partial t} + \boldsymbol{u}\cdot\boldsymbol{\nabla}\boldsymbol{u} = -\boldsymbol{\nabla}\mathcal{H} + \nabla^2\boldsymbol{u} - \frac{L}{Pr}\theta\boldsymbol{g}_e, \tag{4}$$

$$\frac{\partial \theta}{\partial t} + \boldsymbol{u}\cdot\boldsymbol{\nabla}\theta = \frac{1}{Pr}\nabla^2\theta, \tag{5}$$

Table 1. Electric gravity in some dielectric liquids in a capacitor with $d = 10$ mm under an electric voltage $V_0 = 1$ kV and a temperature difference 1 K. The working temperature is 25 °C.

Liquid	ρ (10^3 kg/m^3)	α (10^{-3} K^{-1})	Dielectric constant	e (K^{-1})	$g_{e,0}$ (m/s^2)
Acetonitrile	0.777	1.38	36	0.155	7.11
Nitrobenzene	1.198	0.830	34.9	0.188	10.9
Acetone	0.785	1.43	19.1	0.086	1.11
Chlorobenzene	1.101	0.985	5.61	0.0157	0.0113

coupled with Gauss's law of electricity:

$$\boldsymbol{\nabla} \cdot [(1 - B\theta)\, \boldsymbol{E}_0] = 0 \quad \text{with } \boldsymbol{E}_0 = -\boldsymbol{\nabla}\phi_0. \tag{6}$$

The Bernoulli function $\mathcal{H}$ in eq. (4) involves EHD terms lumped with the hydrodynamic pressure. The viscous dissipation and Joule heating have been neglected in the heat equation (5), following the arguments developed by Yavorskaya *et al.* [20]. The electric field variation in time with $\sin(2\pi f t)$ has been factorized out from the electrostatic law (6). The equation hence concerns only the effective field, which can be computed from the effective electric potential ϕ_0.

Equations (3)–(6) have been nondimensionalized with the following scales: the gap d between the electrodes for the length, the viscous relaxation time $\tau_\nu = d^2/\nu$ for the time, the diffusion velocity ν/d for the velocity, $\Delta\theta$ for the temperature, and V_0/d for the electric field. The Prandtl number $Pr = \nu/\kappa$, the thermoelectric parameter $B = e\Delta\theta$ have been introduced.

The electric Rayleigh number L in eq. (4) is defined by $L = \alpha\Delta\theta g_{e,0} d^3/\kappa\nu$, where $g_{e,0}$ is the time-averaged electric gravity at the middle of the gap:

$$g_{e,0} = \frac{e\epsilon_1 V_0^2 B^3}{\rho\alpha d^3} \left[\log\left(\frac{1 - B/2}{1 + B/2}\right)\right]^{-2}. \tag{7}$$

Table 1 shows some values of $g_{e,0}$ evaluated for different dielectric liquids. The electric gravity in the momentum equation (4) has been scaled by this reference gravity $g_{e,0}$ and is given by the dimensionless expression:

$$\boldsymbol{g}_e = \frac{1}{2B^3} \left[\log\left(\frac{1 - B/2}{1 + B/2}\right)\right]^2 \boldsymbol{\nabla} \left|\boldsymbol{\nabla}\phi_0\right|^2. \tag{8}$$

The boundary conditions at the electrodes ($x = \pm 1/2$) and at the adiabatic walls ($z = \pm\Gamma/2$) for the governing equations (3)–(6) read in the time-averaged description:

$$\boldsymbol{u} = 0, \quad \theta = \tfrac{1}{2}, \quad \phi_0 = 1 \qquad \text{at } x = -\tfrac{1}{2}, \tag{9}$$

$$\boldsymbol{u} = 0, \quad \theta = -\tfrac{1}{2}, \quad \phi_0 = 0 \qquad \text{at } x = \tfrac{1}{2}, \tag{10}$$

$$\boldsymbol{u} = 0, \quad \partial_z\theta = 0, \quad \partial_z\phi_0 = 0 \qquad \text{at } z = \pm\tfrac{\Gamma}{2}. \tag{11}$$

When the electric Rayleigh number L is smaller than a critical value, the homogeneous stationary state $(\boldsymbol{u}, \theta, \phi_0) = (\boldsymbol{0}, \bar{\theta}(x), \bar{\phi}_0(x))$ is established, where

$$\bar{\theta} = -x, \quad \bar{\phi}_0 = \log\left(\tfrac{1+Bx}{1+B/2}\right) \Big/ \log\left(\tfrac{1-B/2}{1+B/2}\right). \tag{12}$$

The electric field $\bar{\boldsymbol{E}}_0$ is computed by $\bar{\boldsymbol{E}}_0 = -(\partial\bar{\phi}_0/\partial x)\boldsymbol{e}_x$, where $\boldsymbol{e}_x$ is the unit vector in the transverse direction (x). The electric gravity $\bar{\boldsymbol{g}}_e$ in this base state is nonuniform and directed from the cold to hot electrodes, i.e., from right to left in fig. 1:

$$\bar{\boldsymbol{g}}_e = \bar{g}_e \boldsymbol{e}_x \quad \text{with } \bar{g}_e = -\frac{1}{(1 + Bx)^3}. \tag{13}$$

In the present work, we consider a two-dimensional system with a large aspect ratio, $\Gamma = 114$, for different values of Pr to simulate the nonlinear behavior of the TEHD convection. The thermoelectric parameter will be set at a small value ($B = 0.03$). The set of partial differential equations (3)–(6) with the boundary conditions (9)–(11) are solved by the finite element method implemented in a commercial software package (COMSOL Multiphysics 3.5, Comsol AB, Stockholm, Sweden). Numerical grids are made of identical rectangles with sides of $\Delta x = 0.1$ and $\Delta z = 0.15$ so that the fluid domain is divided by 10 and 760 along the x and z directions, respectively. The backward differentiation formula is used for the time integration. The convergence of computation was verified by grid refinements. The initial fields are specified as null for the velocities, the temperature, and the electric field: The solved problem corresponds to a situation where the electric potential V_0 and the temperature difference $\Delta\theta$ are imposed at $t = 0$ instantaneously on a steady isothermal fluid layer.

3 Results

Velocity $\boldsymbol{u}'$ $(= u'\boldsymbol{e}_x + w'\boldsymbol{e}_z)$, temperature θ $(= \bar{\theta} + \theta')$ and electric field $\boldsymbol{E}_0$ $(= \bar{\boldsymbol{E}}_0 + \boldsymbol{E}_0')$ have been computed for a given set of parameter values (Pr, B, L). All the obtained data exhibit a supercritical bifurcation from the conductive state to a convective regime with a critical electric Rayleigh number $L_c = 2130$. As Yoshikawa *et al.* [10] have shown, this value is independent of Pr and very close to L_c determined by the linear stability theory (2128.7). The critical modes are stationary and independent of Pr.

Hot and cold fluids are, respectively, convected to the cold and hot electrodes by the thermal buoyancy due to the electric gravity and form convection rolls (fig. 2a,c). The temperature perturbation θ' and the transverse velocity u' are in phase. Perturbation electric fields $\boldsymbol{E}'$ are concentrated on the electrodes (fig. 2e), where the storage

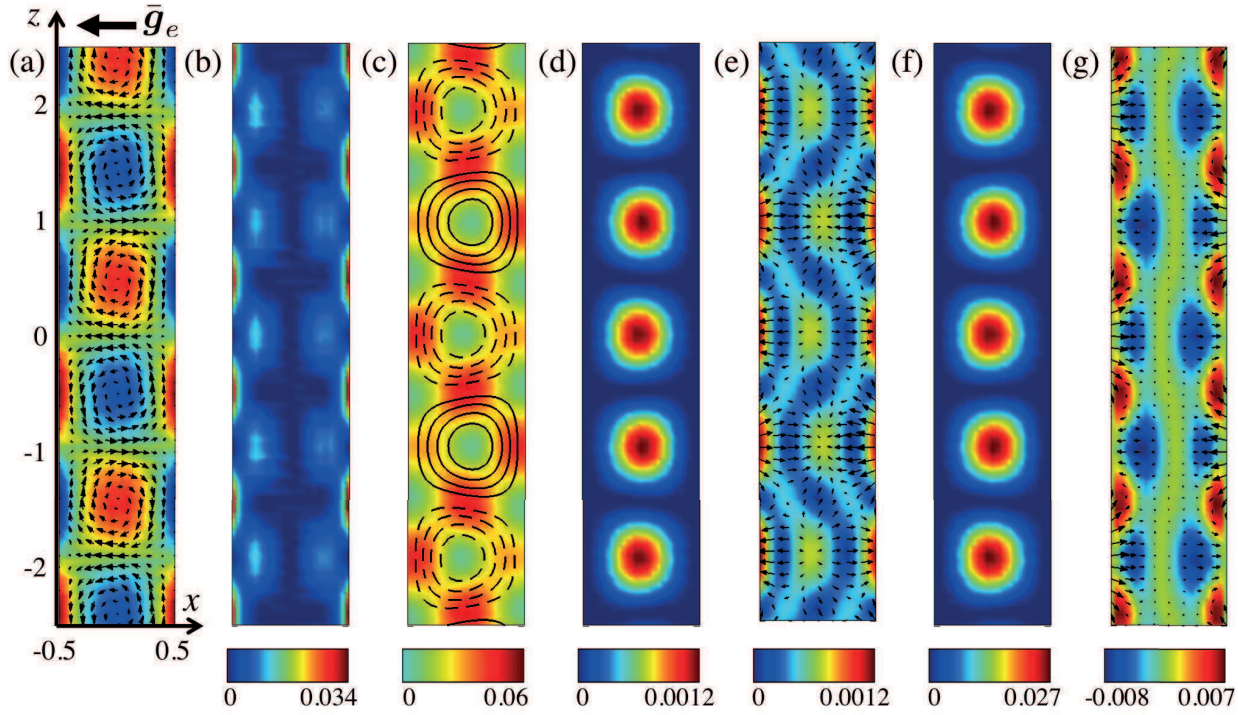

Fig. 2. Saturated flow fields and related quantities at the central part of electrodes ($B = 0.03, Pr = 100, L = 2200$). The basic electric gravity $\bar{\boldsymbol{g}}_e$ is directed from right to left. (a) Velocity vectors $\boldsymbol{u}'$ with vorticity intensity $|\boldsymbol{\nabla} \times \boldsymbol{u}'|$, (b) viscous dissipation function Φ, (c) isotherms $\theta' = const$ (solid and broken lines indicate positive and negative θ', respectively) with thermal dissipation $|\boldsymbol{\nabla}\theta'|^2$, (d) convective heat transfer $\langle u'\theta' \rangle$, (e) electric field intensity $|\boldsymbol{E}_0'|$ with the perturbation electric gravity vectors $\boldsymbol{g}_e'$, (f) power input by the basic electric gravity w_{BG}, (g) power input by the perturbation electric gravity w_{PG} with the buoyancy force vectors, $-Pr^{-1}L(\bar{\theta} + \theta')\boldsymbol{g}_e'$, due to the perturbation electric gravity.

of electrostatic energy might be intensified. This intensification is actually found but only by a tiny quantity compared with the electrostatic energy stored in the base state (fig. 3). This indicates that the convection does not require much additional energy supply for its development.

The perturbation electric gravity $\boldsymbol{g}_e' = g_{e,x}'\boldsymbol{e}_x + g_{e,z}'\boldsymbol{e}_z$ is calculated from the temperature and electric fields (fig. 2 e). The transverse components of the perturbation gravity and velocity, $g_{e,x}'$ and u', are in phase and in antiphase, respectively, in the left and right halves of the fluid layer. Their axial (z) components, $g_{e,z}'$ and w', are in antiphase and in phase, respectively, in the left and right halves of the fluid layer.

In order to gain a better insight into the TEHD convection, we have used the equations of kinetic energy and temperature variance averaged over the flow domain:

$$\frac{d}{dt}\left\langle \frac{1}{2}\boldsymbol{u}'^2 \right\rangle = \langle w_{BG} \rangle + \langle w_{PG} \rangle - \langle \Phi \rangle , \qquad (14)$$

$$\frac{d}{dt}\left\langle \frac{\theta'^2}{2} \right\rangle = \langle u'\theta' \rangle - \frac{1}{Pr}\left\langle |\boldsymbol{\nabla}\theta'|^2 \right\rangle , \qquad (15)$$

where $\langle\ \rangle$ means the average over the whole fluid domain: $\langle\ \rangle = \Gamma^{-1}\iint dxdz$. Different terms w_{BG}, w_{PG} and Φ in the energy equation (14) are the power input by the basic electric gravity, the power input by the perturbation electric gravity and the viscous dissipation function, respectively:

$$w_{BG} = -\frac{L}{Pr}\theta' u' \bar{g}_e, \quad w_{PG} = -\frac{L}{Pr}\left(\bar{\theta} + \theta'\right)\boldsymbol{u}' \cdot \boldsymbol{g}_e' \qquad (16)$$

$$\Phi = 2\left(\frac{\partial u'}{\partial x}\right)^2 + \left(\frac{\partial u'}{\partial z} + \frac{\partial w'}{\partial x}\right)^2 + 2\left(\frac{\partial w'}{\partial z}\right)^2 . \qquad (17)$$

In the temperature variance equation (15), the first term in the RHS represents the convective heat transfer. The second term is the thermal dissipation.

The power input w_{BG} by the basic electric gravity is positive everywhere (fig. 2f), as u' and θ' are in phase and $\bar{g}_e < 0$. The power is concentrated at hot and cold cores. In contrast, the power input w_{PG} by the perturbation electric gravity is null at the middle of the gap (fig. 2 g). It is positive near the electrodes, while it takes negative values inside the gap. In fact, the transverse component of the thermoelectric buoyancy $-Pr^{-1}L(\bar{\theta} + \theta')\boldsymbol{g}_e'$, which produces w_{PG}, is in antiphase with the transverse velocity (fig. 2g). This yields negative w_{PG} zones inside the gap. In contrast, the axial component of the buoyancy is in phase with the axial velocity, but significant only on the electrodes, where the velocity is weak. This results in weak positive power input zones on the electrodes. The viscous dissipation is primarily due to the shear at the electrodes (fig. 2b).

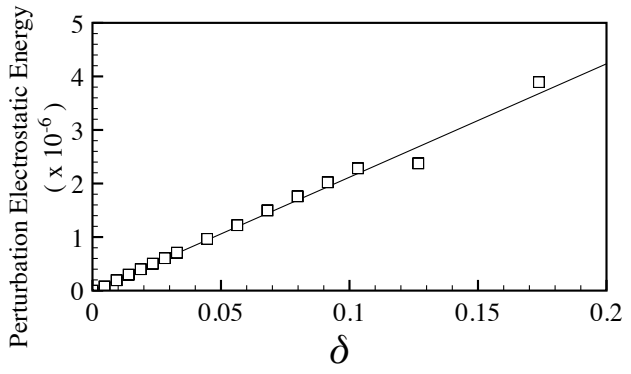

Fig. 3. Electrostatic energy perturbation $\Delta U_E = (\epsilon \boldsymbol{E}_0^2 - \bar{\epsilon}\bar{\boldsymbol{E}}_0^2)/2$ averaged over the whole fluid domain, as a function of the normalized distance from the criticality $\delta = L/L_c - 1$ ($Pr = 100$, $B = 0.03$).

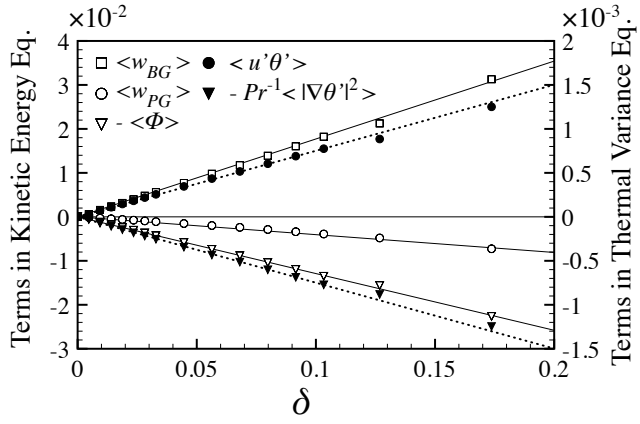

Fig. 4. Different terms in the kinematic energy eq. (14) and in the temperature variance eq. (15), as a function of the normalized distance from the criticality $\delta = L/L_c - 1$ ($Pr = 100$, $B = 0.03$). All the terms were computed after the saturation.

The convective heat transfer $u'\theta'$ is positive everywhere, since u' and θ' are in phase (fig. 2d). It is concentrated in the hot and cold cores. The thermal dissipation $|\boldsymbol{\nabla}\theta'|^2$ occurs in the bulk as well as at the electrodes (fig. 2c), where the convective transfer is weak (fig. 2d).

In the average taken over the whole fluid domain, the basic electric gravity provides energy to the flow, while the perturbation electric gravity impedes the convection. Figure 4 shows different terms in eqs. (14) and (15) for saturated convection as a function of the normalized distance δ from the criticality: $\delta = L/L_c - 1$. A similar result was reported in the preceding work [10] for a different Prandtl number ($Pr = 10$), but only for the terms in the kinetic energy equation (14): the terms $\langle u'\theta' \rangle$ and $-Pr^{-1} \langle |\boldsymbol{\nabla}\theta'|^2 \rangle$ are given for the first time. The latter two terms are balanced with each other, since the convection is in a saturated state.

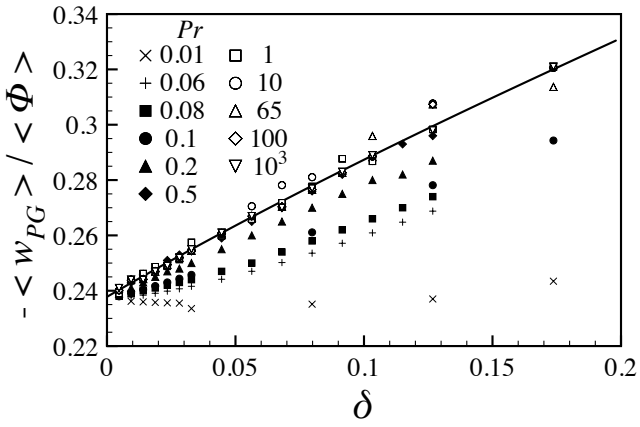

Fig. 5. Relative importance of $\langle w_{PG} \rangle$ to $\langle \Phi \rangle$ computed for saturated convections ($B = 0.03$).

The viscous dissipation $\langle \Phi \rangle$ balances with the contributions, $\langle w_{BG} \rangle$ and $\langle w_{PG} \rangle$, from the different electric gravity components. The ratio of $\langle w_{PG} \rangle$ to $\langle \Phi \rangle$ is independent of the Prandtl number larger than the unity (fig. 5). When the distance from the criticality is small, i.e., as $\delta \to 0$, the ratio converges to the same value for all the examined Pr and can be correlated as:

$$\langle w_{PG} \rangle \,/\, \langle \Phi \rangle = -0.24. \tag{18}$$

The ratio of $\langle w_{BG} \rangle$ to $\langle \Phi \rangle$ is given by $\langle w_{BG} \rangle \,/\, \langle \Phi \rangle = -\langle w_{PG} \rangle \,/\, \langle \Phi \rangle + 1 = 1.24$, since $\langle w_{BG} \rangle + \langle w_{PG} \rangle - \langle \Phi \rangle = 0$ in a saturated state from eq. (14). These results will be used later to derive the correlation between the Nusselt number and the viscous dissipation.

4 Discussion

The heat transfer enhancement is given by the Nusselt number Nu:

$$Nu = 1 + \frac{1}{\Gamma} \int_{-\Gamma/2}^{\Gamma/2} (-\partial_x \theta' + Pr\, u'\theta')\, dz, \tag{19}$$

which compares the convective to conductive heat transfers.

Yoshikawa *et al.* [10] showed that the Nusselt number in saturated TEHD convection is proportional to the distance to the onset as $Nu - 1 = C\delta$ with the proportionality constant $C = 0.78$ for Pr larger than the unity. For small Pr, the constant C varies with Pr (fig. 6), as it does in the RB convection. Seeking a correlation similar to that for the RB convection [21], one can find

$$Nu - 1 = \left(1.28 - \frac{0.0273}{Pr} + \frac{0.0077}{Pr^2}\right)^{-1} \delta, \tag{20}$$

for the TEHD convection. For small Prandtl number, the difference in Nu of these two convections is small (fig. 6).

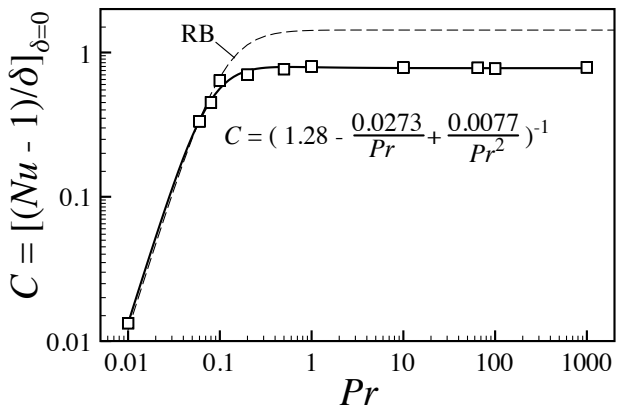

Fig. 6. Proportionality constant C: $Nu-1 = C\delta$, for different Prandtl numbers Pr in the vicinity of the criticality $\delta \approx 0$ ($B = 0.03$). The broken-line curve is the corresponding constant in the Rayleigh-Bénard convection: $C = (0.69942 - 0.00472/Pr + 0.00832/Pr^2)^{-1}$ [21].

In a saturated steady convection, one can show that the Nusselt number Nu can be computed [22] by

$$Nu - 1 = Pr \langle u'\theta' \rangle . \qquad (21)$$

Making use of eq. (15), one finds that $Nu - 1 = \langle |\boldsymbol{\nabla}\theta'|^2 \rangle$, i.e., the heat transfer enhancement is identical to the thermal dissipation. This feature is common in the TEHD convection and in the RB convection, as long as the Joule heating can be neglected in the former one. So, the same thermal dissipation is expected for the same heat transfer in both types of convection.

We can find another similarity between the two types of convection from our simulation results. In the limit of small B, the basic electric gravity (13) is uniform: $\bar{\boldsymbol{g}}_e = -\boldsymbol{e}_x$, so that $w_{BG} = Pr^{-1} L\theta' u'$. Indeed, w_{BG} and $u'\theta'$ are identical in our simulation for $B = 0.03$ except the factor $Pr^{-1}L$ (fig. 2 d,f). The heat transfer (21) can then be computed by

$$Nu - 1 = \frac{Pr}{L} \langle w_{BG} \rangle = \frac{Pr}{L} \left(- \langle w_{PG} \rangle + \langle \Phi \rangle \right) . \qquad (22)$$

Since the ratio of $\langle w_{PG} \rangle$ to $\langle \Phi \rangle$ is given by eq. (18) in the vicinity of the criticality, we have $Nu - 1 = 1.24\, Pr L_c^{-1} \langle \Phi \rangle = Pr \langle \Phi \rangle / 1720$. One can derive a similar relationship for the RB convection: $Nu - 1 = PrR^{-1} \langle \Phi \rangle$ [22,23], which yields $Nu - 1 = Pr \langle \Phi \rangle / 1708$ in the vicinity of the criticality. The same heat transfer in both types of convection in a dielectric fluid is accompanied by the same viscous dissipation.

These results obtained in the vicinity of the criticality indicate that, despite of the difference in the convection mechanism between TEHD and RB flows, the relationships between the heat transfer and the viscous and thermal dissipations are the same in both flows.

5 Conclusion

The thermo-electro-hydrodynamic convection in dielectric fluids represents a simple way of realizing thermal convection under microgravity conditions. We have highlighted the effect of the perturbation gravity against the destabilization induced by the basic electric gravity. The heat transfer by the TEHD convection has been quantified for different values of the Prandtl number. The behavior of the convection has been analyzed in detail from an energetic viewpoint in the vicinity of the criticality and compared with the RB convection to show further similarities between them: the viscous and thermal dissipations are the same in both convective systems to yield the same heat transfer.

This work benefited from a financial support from CNES (French Space Agency), the CPER-Haute Normandie under the program THETE and from the FEDER. M.T.F. thanks the MESR for financial support during her Ph.D preparation. H.N.Y. acknowledges the financial support of the French National Research Agency (ANR), through the program *Investissements d'Avenir* (ANR-10 LABX-09-01), LABEX EMC^3.

References

1. P. Manneville, *Structures dissipatives chaos et turbulence* (CEA, Gif-sur-Yvette, 1991)
2. P. Bergé, Y. Pomeau, C. Vidal, *Order within chaos: Towards a deterministic approach to turbulence* (John Wiley & Sonc Inc., 1986)
3. M.C. Cross, P.C. Hohenberg, Rev. Mod. Phys. **65**(3), 851 (1993)
4. R. Tagg, P.D. Weidman, Z. Angew. Math. Phys. **58**, 431 (2007)
5. B. Chandra, D.E. Smylie, Geophysical Fluid Dynamics **3**, 211 (1972)
6. P.H. Roberts, Q. J. Mech. Appl. Math. **22**, 211 (1969)
7. R.J. Turnbull, Phys. Fluids **12**(9), 1809 (1969)
8. P.J. Stiles, Chem. Phys. Lett. **179**(3), 311 (1991)
9. B.L. Smorodin, Tech. Phys. Lett. **27**(12), 1062 (2001)
10. H.N. Yoshikawa, M.T. Fogaing, O. Crumeyrolle, I. Mutabazi, Phys. Rev. E **87**, 043003 (2013)
11. L.D. Landau, E.M. Lifshitz, *Electrodynamics of Continuous Media*, Vol. 8 of *Landau and Lifshitz Course of Theoretical Physics*, 2nd edn. (Elsevier Butterworth-Heinemann, Burlington, Massachusetts, 1984)
12. J.R. Melcher, *Continuum Electromechanics* (The MIT Press, 1981)
13. T.B. Jones, Adv. Heat Transfer **14**, 107 (1979)
14. M. Takashima, H. Hamabata, J. Phys. Soc. Jpn **53**(5), 1728 (1984)
15. S. Chandrasekhar, *Hydrodynamic and hydromagnetic stability* (Dover, New York, 1961), secs. 7&8
16. P.J. Stiles, F. Lin, P.J. Blennerhassett, Phys. Fluids A **5**(12), 3273 (1993)
17. H.N. Yoshikawa, O. Crumeyrolle, I. Mutabazi, Phys. Fluids **25**, 024106 (2013)
18. M. Takashima, Q. J. Mech. Appl. Math. **33**(1), 93 (1980)
19. B.L. Smorodin, M.G. Velarde, J. Electrostatics **50**(3), 205 (2001)

20. I.M. Yavorskaya, N.I. Fomina, Y.N. Belyaev, Acta Astronaut. **11**(3–4), 179 (1984)
21. A. Schlüter, D. Lortz, F. Busse, J. Fluid Mech. **23**, 129 (1965)
22. E.D. Siggia, Annu. Rev. Fluid Mech. **26**, 137 (1994)
23. B.I. Shraiman, E.D. Siggia, Phys. Rev. A **42**(6), 3650 (1990)